Microsc. Microanal. 19, S5, 99–104, 2013
doi:10.1017/S1431927613012427

# Composition Fluctuation of In and Well-Width Fluctuation in InGaN/GaN Multiple Quantum Wells in Light-Emitting Diode Devices

Gil Ho Gu,[1] Dong Hyun Jang,[1] Ki Bum Nam,[2] and Chan Gyung Park[1,3,*]

[1]*Department of Materials Science and Engineering, Pohang University of Science and Technology (POSTECH), Pohang, 790-784, South Korea*
[2]*Characterization & Analysis Lab, Seoul Opto Device Co., Ansan, 425-851, Korea*
[3]*National Center for Nanomaterials Technology (NCNT), Pohang, Kyungbuk 790-784, South Korea*

**Abstract:** In this paper, we have observed an atomic-scale structure and compositional variation at the interface of the InGaN/GaN multi-quantum wells (MQW) by both scanning transmission electron microscopy (STEM) using high-angle annular dark-field mode and atom probe tomography (APT). The iso-concentration analysis of APT results revealed that the roughness of InGaN/GaN interface increased as the MQW layers were filled up, and that the upper interface of MQW (GaN/InGaN to the *p*-GaN side) was much rougher than that of the lower interface (InGaN/GaN tot he *n*-GaN side). On the basis of experimental results, it is suggested that the formation of interface roughness can affect the quantum efficiency of InGaN-based light-emitting diodes.

**Key words:** composition fluctuation of In, well-width fluctuation, atom probe, STEM, InGaN, LED

## Introduction

InGaN-based multiple quantum well (MQW) structure is generally used as an active layer in various commercial optoelectronic devices, such as light-emitting diodes (LEDs) and laser diodes. This is caused by the easy control of the energy band gap from IR to UV by simply changing the ratio of In and Ga in the InGaN well layer (Nakamura et al., 1995, 1996). The atomic structure, composition, and epitaxial quality of the interface between GaN and InGaN in MQWs can severely influence the optical, electrical, and mechanical properties of the optoelectronic devices (Singh et al., 1984, Singh & Bajaj, 1985). Therefore, accurate structural and chemical information, which can characterize precisely the interface between GaN and InGaN, is very much demanding.

It is known that carrier localization can originate from the compositional fluctuation of In in the InGaN well (Ruterana et al., 2002; Cheng et al., 2004), well-width fluctuation of InGaN (Grandjean et al., 2001; Brandt et al., 2002), and likely growth of quantum dots (Graham et al., 2005); however, these remain poorly understood (Narayan et al., 2002). Although various indirect experimental results have been reported as an evidence of compositional fluctuation or In clustering in nm scale (Jinschek et al., 2006; Van der Laak et al., 2007), the problems still remain to be solved. To observe the compositional localization phenomenon as direct evidence, high-resolution transmission electron microscopy (HRTEM) and scanning transmission electron microscopy (STEM) using high-angle annular dark-field (HAADF) mode have been used with their high spatial resolution. Results on the existence of In fluctuation or clustering can, however, be questioned because of an extreme sensitivity of InN under accelerated electron beam doses (O'Neill et al., 2003; Smeeton et al., 2006). Therefore, a separate direct method to characterize the compositional fluctuation of In in the atomic scale is quite required. Indeed, we already reported the fluctuation of In composition to form nanometer-scale clusters in the InGaN well layer (Gu et al., 2009). Atom probe tomography (APT) allows us to analyze the individual atoms that can provide structural and compositional information in a subnanometer spatial resolution (Miller, 1986).

In this paper, we are going to discuss the relationship between the compositional fluctuation of In in InGaN wells in MQWs and the interface roughness between the GaN and InGaN layers, based on the results obtained by APT.

## Methods and Materials

All samples were commercially available InGaN-based blue LEDs obtained from various manufacturers. The MQW structure was grown on *c*-plane (0001) sapphire substrates by metal-organic vapor-phase epitaxy. To analyze the cross-sectional microstructure of InGaN/GaN MQWs, cross-sectional TEM specimens and needle-type APT specimens with a radius of curvature $<$50 nm were prepared by using a focused ion beam (FIB; Gu et al., 2009). To minimize any surface damage associated with Ga ions during initial rough milling at 30 kV, the samples were protected by a 100-nm-thick sputter-deposited Ni layer and a 2-$\mu$m-thick ion-beam-induced Pt layer deposited in the FIB. In addition, the sample was milled in the final stage at a low acceleration voltage of 1–5 kV for a few minutes. The MQWs, which are about 100 nm in depth, should be positioned at the APT tip within the apex region of the needle-shaped specimen. Therefore, the height from the surface to the AlGaN layer


*Corresponding author. E-mail: cgpark@postech.ac.kr

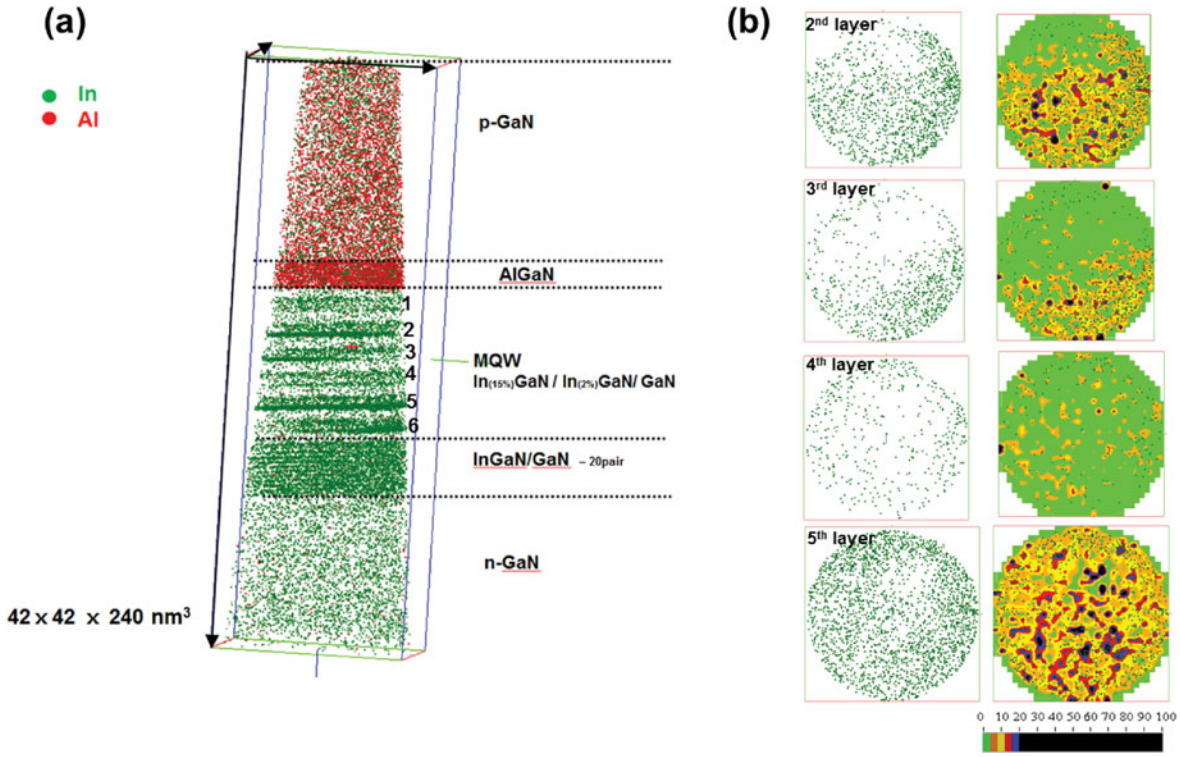


**Figure 1. a:** The atom probe tomography image of the light-emitting diode device from *p*-GaN to *n*-GaN: the red dots represent Al atoms and green dots represent In atoms. **b:** In maps of individual quantum wells and corresponding In concentration maps, which are color coded for concentration level.

was measured by high-resolution electron microscopy because the available sampling depth for the APT analysis is usually very small (200 nm). The APT samples were analyzed with a laser-assisted wide-angle tomographic atom probe (CAMECA-LAWATAP) and a local electrode atom probe (LEAP$^{TM}$ 4000X HR). For controlled evaporation of atoms, the LAWATAP experiment was carried out with green-laser pulse of 360 fs duration and the repetition rate of 10 kHz at a cryogenic temperature of 50–60 K. On the other hand, the Leap experiment was performed, the specimens were cooled to a base temperature of 20 K, and a standing voltage between 5.5 and 9 kV was applied. An ultrafast pulsed laser (~10 ps) with a 355 nm wavelength at 250 kHz pulse repetition was applied. The average detection rate amounted to 0.02 atoms/pulse. The APT results were compared with the results obtained by HRTEM and STEM-HAADF operated at 200 kV in a JEM 2100F equipped with a probe $C_s$ corrector. The orientation of the cross-sectional TEM specimen was identical to that of the APT tip along the $[11\bar{2}0]$ zone axis.

## Results and Discussion

### Lateral Distribution of the In in Quantum Well Layer

The APT image shown in Figure 1 revealed the structure and composition information of the LED device. The results clearly revealed each InGaN QW layer with GaN barrier layer with a color-coded elemental map of dimensions $42 \times 42 \times 1$ nm$^3$. The Al and In atoms are shown in red and green, respectively. The areas selected are indicated from the second layer to the fifth layer, respectively. In order to investigate the density and size of the compositional fluctuation of In in an InGaN well layer, two-dimensional iso-concentration analysis was performed, as shown in Figure 1b. Although three-dimensional atom maps, shown in Figure 1a, can show the distribution and positional information of an individual element, they cannot display the exact compositional variation of a specific area. Therefore, it is difficult to state whether In clusters or In-rich regions in the InGaN well layer were formed or not. On the other hand, the two-dimensional iso-concentration map can clearly show the variation in size and density of In clusters or In-rich regions at a specific region (cf., the *x*–*y* plane). Thus, using this method, we can display and analyze the different In compositions with different colors. Six different colors were used to identify the size and morphology of In clustering or In-rich regions in the ranges of 0–4, 4–8, 8–12, 12–16, 16–20, and >20 at.%. One can see that the InGaN well layer has a severe uniformity. In fact, the InGaN well layer must be formed of uniform well widths and element compositions. However, even the In atoms were nearly nonexistent (under 0.5 at.%) in certain areas.

Figure 2b shows a schematic diagram of the relationship between the interface roughness and In-rich regions. The width of interface roughness, *L*, is related to the role of interface characterization. Interface roughness is important when strong piezoelectric field exists at the MQWs, which

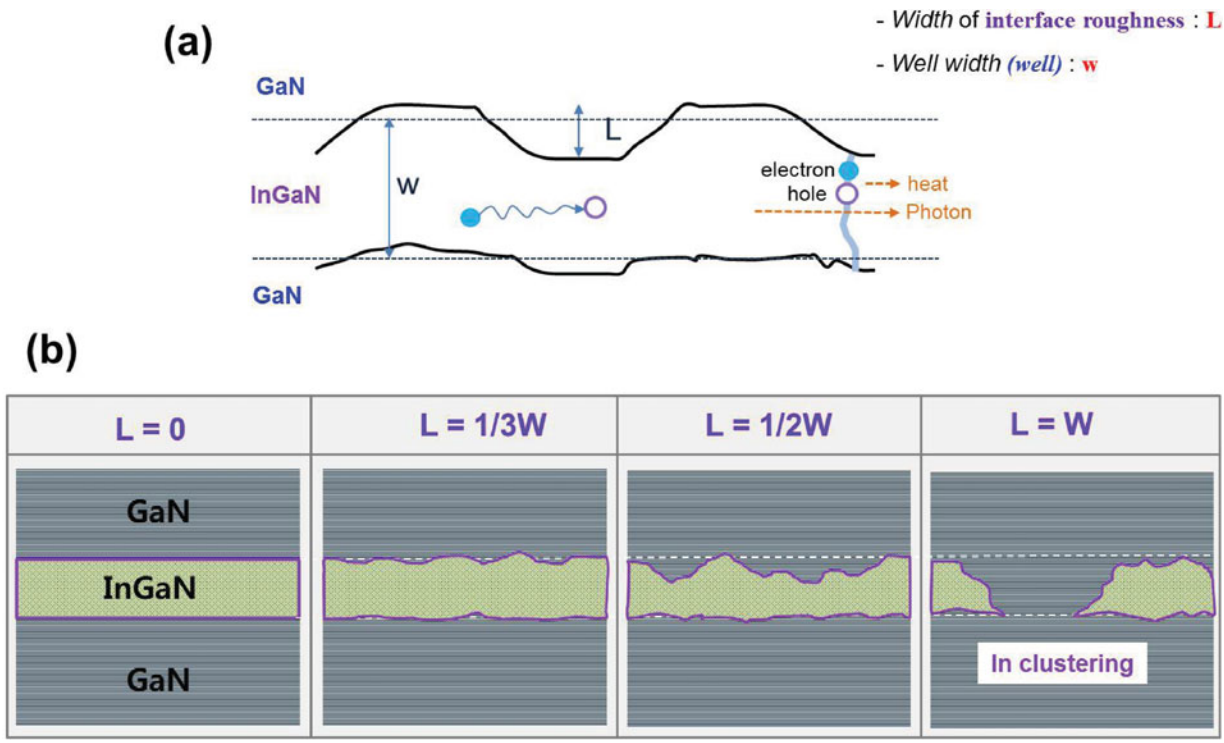


**Figure 2.** **a:** Schematic diagram of well-width fluctuation at a single quantum well. **b:** Shape of the InGaN well layer depending on the width of interface roughness *L*.

affects the carrier density on the position of InGaN well layer. Generally, the width of a quantum well (InGaN) is in the range of 2.5–3 nm. In the case where *L* is nearly zero, the thickness of the InGaN well layer is identical to that of the designed well layer. However, this is practically impossible owing to alloy disorders and induced strains by lattice mismatches between the GaN and InGaN layers. Thus, the width of the interface roughness is affected by various factors such as growth condition, residual strain, and In composition. Thus, when *L* is close to the InGaN well width *W*, the InGaN well layer has a very rough interface and many discontinuous InGaN layers or In clustering. It is known that such interface roughness and In clustering decrease the diffusion length and nonradiative recombination rate because of interface roughness scattering (Singh & Singh, 2003; Lu et al., 2010).

Figures 3a and 3b show the HAADF images of a single QW at a rough interface region and comparatively flat interface region. To visualize a clear difference in the GaN and InGaN boundary, HAADF images were color coded depending on the image intensity. As shown in Figure 3a, the width of interface roughness, *L*, was found to be close to the value of the well width, *w*. In contrast, the *L* was nearly zero in the flat interface region, as shown in Figure 3b.

## Well-Width Fluctuation of the Interface between GaN and InGaN

We exploited cross-sectional STEM imaging of the MQW structure to visualize the discontinuous In layer directly, because the contrast of STEM-HAADF images is highly

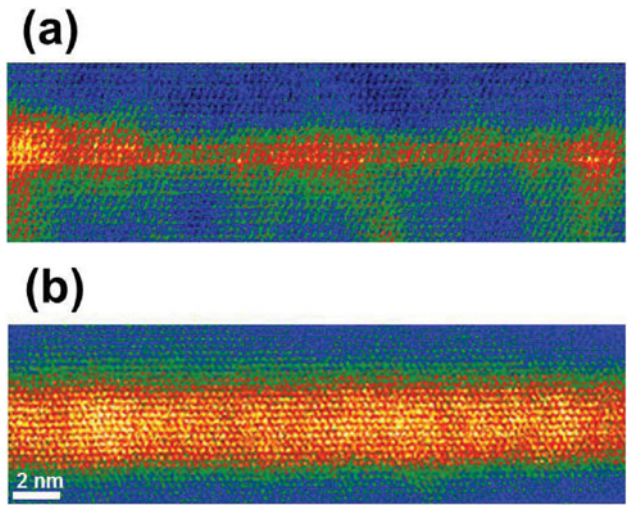


**Figure 3.** Cross-sectional scanning transmission electron microscopy high-angle annular dark-field images of single quantum well layer (**a**) width of interface *L* is large and (**b**) nearly zero.

sensitive to the atomic number ($Z$). The difference in contrast between In ($Z = 49$) and Ga ($Z = 31$) is generated by the difference in atomic number. Figure 4a shows a cross-sectional STEM-HAADF image obtained from MQWs composed of InGaN and GaN, viewed along their common $[11\bar{2}0]$ zone axis. The interface between InGaN and GaN is clearly observed because In is heavier than Ga or N. An InGaN surface (i.e., the interface between GaN/InGaN) tends to maintain an intrinsic roughness owing to local alloy fluctuations or processes characteristic of the growth

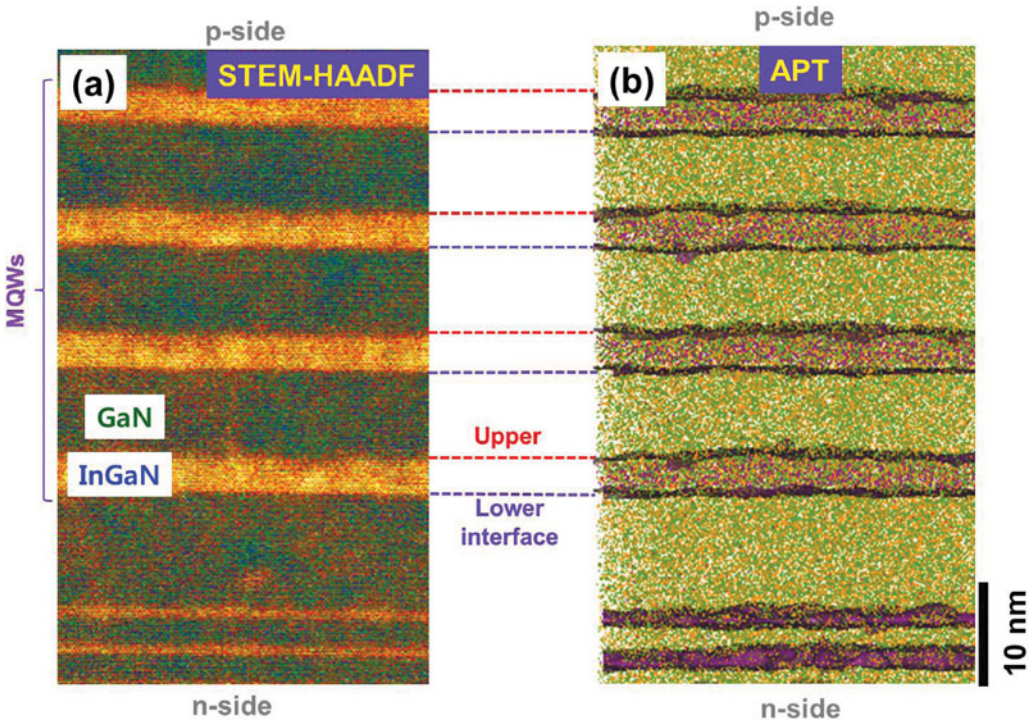


**Figure 4.** **a:** Cross-section of STEM-HAADF image showing the active region. **b:** Cross-section atom map using 2 at.% isoconcentration surface analysis for In. STEM, scanning transmission electron microscopy; HAADF, high-angle annular dark-field; MQW, multiple quantum well; APT, atom probe tomography.

in MOCVD. In contrast, a GaN surface (i.e., the interface between InGaN/GaN) tends to be more regular. Consequently, an interface between InGaN/GaN (the lower interface) will be flatter than that originating from the InGaN well layer (the upper interface). This assumption was further verified by the APT analysis in Figure 4b, which shows a color-coded elemental atomic map. The Ga, N, and In atoms are shown in dark orange, dark green, and violet, respectively. The atomic map in Figure 4b shows a local view of the center of the entire analysis volume ($90 \times 90 \times 150$ nm$^3$). The violet isosurface indicates 2 at.%. The interior atomic composition of In at MQWs is measured as 6.6–7.2 at.%. The isoconcentration analysis shows that the roughness of the interface is clearly identified by the 2 at.% isoconcentration surface; the boundary of a QW divided by this isoconcentration surface exhibits a very abrupt change (Galtrey et al., 2008).

To measure this interface characteristic directly, we analyzed the root mean square (RMS) roughness of each QW from the *n*-GaN to the *p*-GaN substrate. Figure 5b shows the RMS roughness as a function of the position from the *n*-GaN substrate. Clearly, the RMS roughness of the upper interface is higher than that of the lower interface. The ranges of RMS roughness for the upper and lower interfaces are 0.337–0.466 and 0.224–0.316 nm, respectively. In particular, the RMS roughness of the upper interface gradually increases from 0.349 to 0.466 nm going from the *n*-GaN to the *p*-GaN substrate.

These characteristics of the interface roughness are crucial because the recombination of electrons and holes generally occurs at the QW near the *p*-GaN substrate; that is, the efficiency of radiative recombination could be a result of the interface roughness due to the residual strain between the GaN and InGaN layer. It is generally known that differences in interface roughness arise from the presence of a residual In precursor (trimethyl In) during growth of the GaN barrier layer by MOCVD (Northrup & Van de Walle, 2004). However, if this precursor is solely responsible for increasing the roughness of the upper interface, the interface roughness of each QW must be within the limits of error. The present results suggest that there is another contribution to the interface roughness, such as the effects of alloy disordering. In addition, GaN and InN have the hexagonal wurtzite structure with a large latticed mismatch around ~10.6% on the basal plane. It has been reported that in most cases this misfit strain cannot be relaxed, and thus, the pseudomorphic structure of the InGaN/GaN quantum well layer can reveal the residual strain. Therefore, it is suggested that the upper interface has a larger roughness than the lower interface, due to the accumulated strain in InGaN well during growth.

## Conclusion

In conclusion, we have observed various types of InGaN well layers in terms of interface roughness and differences in interface characteristics as a function of position at the MQWs by STEM-HAADF and APT. The well-width fluctuation of the interface between GaN and InGaN was investigated from the thickness of the monolayer (one or two

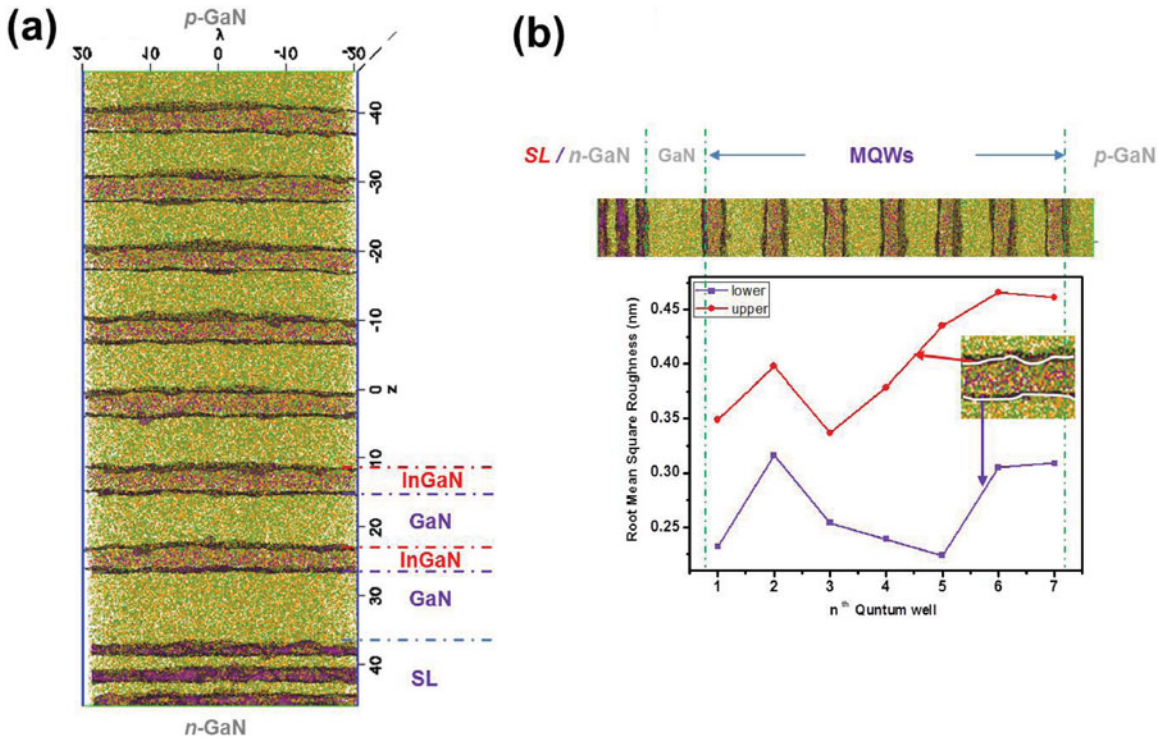


**Figure 5.** **a:** Cross-section of an atom map at multiple quantum wells (MQWs) measured by using 2 at.% isoconcentration surface for In. **b:** Root mean square roughness depending on the position of the quantum well.

monolayers) up to that of the InGaN well layer ($L \approx W$). The RMS roughness of the upper interface gradually increases from 0.349 to 0.466 nm at the *p*-GaN, and the upper interface is rougher than the lower interface. These characteristics of interface roughness are crucial because the recombination of electrons and holes generally occurs at the QW near the *p*-GaN, and the carrier will move across the surface of the InGaN well layer by a strong piezoelectric field. By comparing the APT and STEM-HAADF of the interface, we have shown that the type of structural interface is determined by the size of the well-width fluctuation *L*. These various types of interface could contribute in complex ways to efficient MQW structures.

## Acknowledgments

This research was supported by the Seoul Opto Device and BK 21. The authors want to thank B.H. Lee (NCNT) and CAMECA for the support of facilities.

## References

Brandt, O., Waltereit, P., Jahn, U., Dhar, S. & Ploog, K.H. (2002). Impact of In bulk and surface segregation on the optical properties of (In, Ga) N/GaN multiple quantum wells. *Physica Status Solidi A* **192**(1), 5–13.

Cheng, Y.C., Lin, E.C., Wu, C.M., Yang, C.C., Yang, J., Rosenauer, R.A., Ma, K.J., Shi, S.C., Chen, L.C. & Pan, C.C. (2004). Nanostructures and carrier localization behaviors of green-luminescence InGaN/GaN quantum-well structures of various silicon-doping conditions. *Appl Phys Lett* **84**, 2506–2508.

Galtrey, M.J., Oliver, R.A., Kappers, M.J., Humphreys, C.J., Clifton, P.H., Larson, D., Saxey, D.W. & Cerezo, A. (2008). Three-dimensional atom probe analysis of green-and blue-emitting InxGa1-xN/GaN multiple quantum well structures. *J Appl Phys* **104**(1), 013524–013527.

Graham, D.M., Soltani-Vala, A., Dawson, P., Godfrey, M.J., Smeeton, T.M., Barnard, J.S., Kappers, M.J., Humphreys, C.J. & Thrush, E.J. (2005). Optical and microstructural studies of InGaN/GaN single-quantum-well structures. *J Appl Phys* **97**, 103508.

Grandjean, N., Damilano, B. & Massies, J. (2001). Group-III nitride quantum heterostructures grown by molecular beam epitaxy. *J Phys: Condens Matter* **13**, 6945.

Gu, G.H., Park, C.G. & Nam, K.B. (2009). Inhomogeneity of a highly efficient InGaN based blue LED studied by three dimensional atom probe tomography. *Physica Status Solidi (RRL)-Rapid Res Lett* **3**(4), 100–102.

Jinschek, J.R., Erni, R., Gardner, N.F., Kim, A.Y. & Kisielowski, C. (2006). Local indium segregation and bang gap variations in high efficiency green light emitting InGaN/GaN diodes. *Solid State Commun* **137**(4), 230–234.

Lu, I.L., Wu, Y.R. & Singh, J. (2010). A study of the role of dislocation density, indium composition on the radiative efficiency in InGaN/GaN polar and nonpolar light-emitting diodes using drift-diffusion coupled with a Monte Carlo method. *J Appl Phys* **108**, 124508.

Miller, M.K. (1986). Atom probe field ion microscopy. Annual joint meeting of the Electron Microscopy Society of America and the Microbeam Analysis Society.

Nakamura, S., Senoh, M., Iwasa, N. & Nagahama, S. (1995). High-brightness InGaN blue, green and yellow light-emitting diodes with quantum well structures. *Jpn J Appl Phys Part 2 Lett* **34**, 797–799.

Nakamura, S., Senoh, M., Nagahama, S.I., Iwasa, N., Yamada, T., Matsushita, T., Kiyoku, H. & Sugimoto, Y. (1996). InGaN-based multi-quantum-well-structure laser diodes. *Jpn J Appl Phys* **35**(1B), L74–L76.

Narayan, J., Wang, H., Ye, J., Hon, S.J., Fox, K., Chen, J.C., Choi, H.K. & Fan, J.C.C. (2002). Effect of thickness variation in high-efficiency InGaN/GaN light-emitting diodes. *Appl Phys Lett* **81**, 841–843.

Northrup, J.E. & Van de Walle, C.G. (2004). Indium versus hydrogen-terminated GaN (0001) surfaces: Surfactant effect of indium in a chemical vapor deposition environment. *Appl Phys Lett* **84**, 4322–4324.

O'Neill, J.P., Ross, I.M., Cullis, A.G., Wang, T. & Parbrook, P.J. (2003). Electron-beam-induced segregation in InGaN/GaN multiple-quantum wells. *Appl Phys Lett* **83**(10), 1965–1967.

Ruterana, P., Kret, S., Vivet, A., Maciejewski, G. & Dluzewski, P. (2002). Composition fluctuation in InGaN quantum wells made from molecular beam or metalorganic vapor phase epitaxial layers. *J Appl Phys* **91**(11), 8979–8985.

Singh, J. & Bajaj, K. (1985). Role of interface roughness and alloy disorder in photoluminescence in quantum well structures. *J Appl Phys* **57**(12), 5433–5437.

Singh, J., Bajaj, K.K. & Chaudhuri, S. (1984). Theory of photoluminescence line shape due to interfacial quality in quantum well structures. *Appl Phys Lett* **44**(8), 805–807.

Singh, M. & Singh, J. (2003). Design of high electron mobility devices with composite nitride channels. *J Appl Phys* **94**, 2498–2506.

Smeeton, T.M., Humphreys, C.J., Barnard, J.S. & Kappers, M.J. (2006). The impact of electron beam damage on the detection of indium-rich localisation centres in InGaN quantum wells using transmission electron microscopy. *J Mater Sci* **41**(9), 2729–2737.

Van der Laak, N.K., Oliver, R.A., Kappers, M.J. & Humphreys, C.J. (2007). Characterization of InGaN quantum wells with gross fluctuations in width. *J Appl Phys* **102**, 013513.